

The properties of brown dwarfs and low-mass hydrogen-burning stars formed by disc fragmentation

Dimitris Stamatellos[★] and Anthony P. Whitworth

School of Physics & Astronomy, Cardiff University, Cardiff CF24 3AA

Accepted 2008 October 9. Received 2008 October 3; in original form 2008 July 24

ABSTRACT

We suggest that a high proportion of brown dwarf (BD) stars are formed by gravitational fragmentation of massive extended discs around Sun-like primary stars. We argue that such discs should arise frequently, but should be observed infrequently, precisely because they fragment rapidly. By performing an ensemble of radiation-hydrodynamic simulations, we show that such discs typically fragment within a few thousand years, and produce mainly BD stars, but also planetary-mass (PM) stars and very low-mass hydrogen-burning (HB) stars. Subsequently most of the lower mass stars (i.e. the PM and BD stars) are ejected by mutual interactions. We analyse the statistical properties of these stars, and compare them with observations.

After a few hundred thousand years the Sun-like primary is typically left with a close low-mass HB companion, and two much wider companions: a low-mass HB star and a BD star, or a BD–BD binary. The orbits of these companions are highly eccentric, and not necessarily coplanar, either with one another, or with the original disc. There is a BD desert extending out to at least ~ 100 au; this is because BDs tend to be formed further out than low-mass HB stars, and then they tend to be scattered even further out, or even into the field.

BDs form with discs of a few Jupiter masses and radii of a few tens of au, and they are more likely to retain these discs if they remain bound to the primary star. Binaries form by pairing of the newly formed stars in the disc, giving a low-mass binary fraction of ~ 0.16 . These binaries include close and wide BD/BD binaries and BD/PM binaries. Binaries can be ejected into the field and survive, even if they have quite wide separations. BDs that remain as companions to Sun-like stars are more likely to be in BD/BD binaries than are BDs ejected into the field. The presence of close and distant companions around Sun-like stars may inhibit planet formation by core accretion.

We conclude that disc fragmentation is a robust mechanism for BD formation. Even if only a small fraction of Sun-like stars host the required massive extended discs, this mechanism can produce all the PM stars observed, most of the BD stars and a significant proportion of the very low-mass HB stars.

Key words: accretion, accretion discs – hydrodynamics – radiative transfer – methods: numerical – stars: formation – stars: low-mass, brown dwarfs.

1 INTRODUCTION

Brown dwarfs were predicted theoretically by Kumar (1962) and Hayashi & Nakano (1963). They were first detected more than thirty years later (Nakajima et al. 1995; Oppenheimer et al. 1995; Rebolo, Zapatero-Osorio & Martin 1995). Since then hundreds have been

observed, both in nearby young star clusters and in the field (see Luhman et al. 2007, and references therein).

A distinction is often made between brown dwarfs below, and stars above, the H-burning limit at $\sim 80 M_J$ (where $M_J = 2 \times 10^{30}$ g is the mass of Jupiter). Similarly, a distinction is often made between planetary-mass objects below, and brown dwarfs above, the deuterium-burning limit at $\sim 13 M_J$. However, in the context of star formation, these distinctions are – at best – unhelpful.

We will therefore refer collectively to all objects forming by gravitational instability, on a dynamical time-scale, as *stars*. Within

[★]E-mail: D.Stamatellos@astro.cf.ac.uk

Table 1. Nomenclature.

Term	Meaning
Star	Pressure-supported object forming on a dynamical time-scale, by gravitational instability.
Planet	Pressure-supported object forming on a much longer than dynamical time-scale, by core accretion.
HB	Hydrogen-burning star, $M_* \geq 80 M_J$.
BD	Brown dwarf star, $13 M_J \leq M_* \leq 80 M_J$.
PM	Planetary-mass star, $M_* \leq 13 M_J$.
ur-star	Star at the centre of the ur-disc; present from the start of the simulation, and provides the background gravitational and radiation fields.
ur-disc	Disc around the ur-star; the material whose dynamics is to be simulated.
ur-system	ur-star plus ur-disc.

this definition, we will label as hydrogen-burning stars (HBs) those stars with masses above the H-burning limit, as brown dwarf stars (BDs) those stars with masses between the H-burning limit and the D-burning limit and as planetary-mass stars (PMs) those stars with masses below the D-burning limit. This nomenclature is summarized in Table 1. Since there are only three PMs formed in our simulations, we will, for statistical purposes, sometimes lump the PMs in with the BDs.

We note that for very low-mass stars the dynamical time-scale is essentially the freefall time-scale at rather high density. Therefore, it is very short, specifically

$$t_{\text{FF}} \simeq \frac{GM}{10c_s^3} \simeq 0.06 \text{ kyr} \left(\frac{M}{M_J} \right), \quad (1)$$

where we have estimated the freefall time at the centre of a marginally unstable isothermal sphere, and $c_s = 0.2 \text{ km s}^{-1}$ is the isothermal sound speed for molecular gas at $T \sim 10 \text{ K}$. Therefore, the formation of PMs, BDs and low-mass HBs (say below $\sim 200 M_J$) is extremely rapid ($t_{\text{FF}} \lesssim 10 \text{ kyr}$).

In contrast to our definition of stars, we will refer to all objects which form by core accretion, on a much longer time-scale ($\gtrsim 1000 \text{ kyr}$), as planets.

With these definitions, we can discuss a single coherent stellar initial mass function (IMF) which extends below the H- and D-burning limits. This stellar IMF is bounded by a minimum stellar mass, which is determined by the requirement that a star-forming condensation is able to radiate away, on a dynamical time-scale, the PdV work done by compression. This requirement is usually called the opacity limit, but see Masunaga & Inutsuka (1999). For contemporary star formation, in the solar vicinity, the minimum stellar mass is estimated to lie in the range from 1 to $7 M_J$ (Low & Lynden-Bell 1976; Rees 1976; Boyd & Whitworth 2005; Whitworth & Stamatellos 2006).

Given this low minimum stellar mass, it is very likely that the stellar IMF overlaps the planetary-mass function in the interval between 1 and $10 M_J$. However, with the definitions above, the two mass functions are distinct in their origin.

During the last decade there has been much speculation about the origin of BDs (see review by Whitworth et al. 2007). Currently there are three main theories proposed: (i) magnetoturbulent or gravoturbulent fragmentation, (ii) premature ejection of protostellar embryos from their natal cores and (iii) disc fragmentation.

Padoan & Nordlund (2004) suggest that magnetoturbulent fragmentation of molecular clouds produces pre-stellar cores of brown dwarf mass with densities high enough for them to be gravitationally unstable and collapse. Their model follows the standard paradigm of low-mass star formation, i.e. a pre-stellar core collapses to form a single star. The model does not attempt to explain the formation of BDs in clusters and binaries. Additionally, the highly coordinated supersonic velocities needed for these dense low-mass pre-stellar cores to form have yet to be observed.

Gravoturbulent fragmentation of collapsing pre-stellar cores may also produce BDs. Simulations (e.g. Bate, Bonnell & Bromm 2003; Goodwin, Whitworth & Ward-Thompson 2004a,b, 2006) of collapsing turbulent cores produce both HBs and BDs, with numbers in good agreement with observation. However, these simulations have been performed with a barotropic equation of state, and therefore the effects of radiative transfer (e.g. Boss et al. 2000; Whitehouse & Bate 2006; Stamatellos et al. 2007a) are not properly captured.

The ejection scenario is closely associated with the gravoturbulent fragmentation mechanism. In numerical simulations of collapsing turbulent cores, BDs frequently form when protostellar embryos (i.e. very low-mass protostars which have just formed) are ejected from their natal cores due to dynamical interactions with other protostars. As a consequence of ejection they stop accreting, and so they never acquire sufficient mass to sustain hydrogen burning (Reipurth & Clarke 2001).

BDs can also form by disc fragmentation (e.g. Whitworth & Stamatellos 2006; Stamatellos, Hubber & Whitworth 2007b). There are two conditions which must be met for a disc to fragment. First, the disc must be massive enough so that locally gravity can overcome thermal and centrifugal support (Toomre 1964), i.e.

$$Q(R) \equiv \frac{c(R)\kappa(R)}{\pi G \Sigma(R)} \lesssim 1; \quad (2)$$

here Q is the Toomre parameter, c is the sound speed, κ is the epicyclic frequency and Σ is the surface density. Secondly, the disc must cool efficiently so that protocondensations forming in the disc do not simply undergo an adiabatic bounce and dissolve. Both theory and simulations (Gammie 2001; Johnson & Gammie 2003; Rice et al. 2003; Mayer et al. 2004; Mejía et al. 2005; Rice, Lodato & Armitage 2005; Stamatellos, Hubber & Whitworth 2007b) indicate that for disc fragmentation to occur, the cooling time must satisfy

$$t_{\text{COOL}} < \mathcal{C}(\gamma) t_{\text{ORB}}, \quad 0.5 \lesssim \mathcal{C}(\gamma) \lesssim 2.0; \quad (3)$$

here t_{ORB} is the local orbital period, and γ the adiabatic exponent. Numerical simulations suggest that disc fragmentation produces BDs, PMs and also low-mass HBs (Stamatellos et al. 2007b). These objects may either remain bound to the primary star, or be ejected into the field. The main concern with this model is whether massive extended discs actually form in the first place. Observations of such discs are difficult, since they are short lived and heavily embedded in their parental clouds. We return to this issue below.

Two other mechanisms that might form BDs are the photoerosion of massive pre-stellar cores by nearby ionizing stars (Whitworth & Zinnecker 2004), and fragmentation during the second collapse, i.e. when H_2 dissociates (Whitworth & Stamatellos 2006). The former mechanism can only operate in the vicinity of a massive star, and therefore it cannot be a major source of BDs. The latter mechanism has been advocated on theoretical grounds, but it has not yet been shown to work by numerical simulations (e.g. Bate 1998; Stamatellos et al. 2007a).

The above BD formation mechanisms are not exclusive of each other and can work in conjunction in star-forming regions. For

example, gravoturbulent fragmentation can generate cores which collapse to form discs, the discs may then fragment to produce BDs, and the BDs may avoid accreting additional mass by being ejected.

Since all these mechanisms should produce both BDs and low-mass HBs, we expect there to be a continuity in their statistical properties across the H-burning limit, and this is indeed what seems to be observed. Like low-mass HBs, young BDs have discs [and all the consequences thereof, i.e. infrared (IR) excesses, signatures of magnetospheric accretion, X-rays, outflows etc.], they are sometimes found in binary and higher multiple systems, and they co-exist with stars (e.g. Luhman et al. 2007, and references therein).

None the less, some authors (e.g. Thies & Kroupa 2007) find observational evidence that BDs form in a different way to HBs. In this regard the most critical factor is the *brown dwarf desert*, i.e. the lack of close BD companions to Sun-like stars. Radial velocity surveys have revealed a large number of planets orbiting close to Sun-like stars, as well as a large number of low-mass HBs, but very few BDs (Marcy & Butler 2000; see Burgasser et al. 2007 for review). As we shall show below, the brown dwarf desert finds a natural explanation in the mechanics of disc fragmentation and subsequent protostellar dynamics.

In this paper we explore the fragmentation of a disc having comparable mass to the central primary star. In Section 2 we discuss the numerical methods we use, and in Section 3 we describe the initial disc configuration. In Section 4 we present in detail one of the simulations performed, and then describe an ensemble of simulations. In Section 5 we discuss the statistical properties of the stars produced by disc fragmentation and compare them with the observed properties of BDs and low-mass HBs. In Section 6 we describe what observers might expect to see if they observe a fragmented disc after a few hundred years, and in Section 7 we discuss the implications of the disc fragmentation mechanism for planet formation. Finally, in Section 8 we summarize our results.

2 NUMERICAL METHOD

The evolution of the disc is initially followed using smoothed particle hydrodynamics (SPH), until 70 to 80 per cent of the disc mass has been accreted, either on to the stars condensing out of the disc, or on to the central primary star; this typically takes 10 to 20 kyr. Then the residual gas is ignored and the long-term dynamical evolution of the resulting ensemble of stars is followed up to 200 kyr, using a N -body code.

For the hydrodynamics we use the SPH code DRAGON (e.g. Goodwin et al. 2004a,b), which invokes an octal tree (to compute gravity and find neighbours), adaptive smoothing lengths, multiple particle time-steps and a second-order Runge–Kutta integration scheme. The code uses time-dependent viscosity with parameters $\alpha^* = 0.1$, $\beta = 2\alpha$ (Morris & Monaghan 1997) and a Balsara switch (Balsara 1995), so as to reduce artificial shear viscosity (Artymowicz & Lubow 1994; Lodato & Rice 2004; Rice et al. 2005). The smoothing lengths are adapted so that each particle has exactly $N_{\text{NEIB}} = 50$ neighbours; this reduces numerical diffusion to a minimum (Attwood, Goodwin & Whitworth 2007). Sinks are created wherever a bound condensation forms and its density exceeds $\rho_{\text{SINK}} = 10^{-9} \text{ g cm}^{-3}$. SPH particles are accreted on to a sink if they are within $R_{\text{SINK}} = 1 \text{ au}$ of the sink and bound to it. Sinks are identified with stars. We note that our high value of ρ_{SINK} makes the use of sinks relatively safe.

The energy equation and associated radiative transfer are treated with the method of Stamatellos et al. (2007a). This method takes

into account compressive heating or expansive cooling, viscous heating, radiative heating by the background and radiative cooling. The method does not solve the radiation transfer equation (which is unfeasible in hydrodynamic simulations with the current computing resources), but it is an approximate method that performs well, in the optically thin, intermediate and optically thick regimes, and has been extensively tested (Stamatellos et al. 2007a). In particular it reproduces the detailed three-dimensional (3D) results of Boss & Bodenheimer (1979), Boss & Myhill (1992), Masunaga & Inutsuka (2000), Whitehouse & Bate (2006) and also the analytic test of Spiegel (1957). It also performs well in the analytic test of Hubeny (1990) for disc geometries. It is easy to implement in particle- and grid-based codes, and highly efficient (incurring only a 3 per cent overhead, in comparison with simulations performed using a barotropic equation of state).

The gas is assumed to be a mixture of hydrogen and helium. We use an equation of state (Black & Bodenheimer 1975; Masunaga, Miyama & Inutsuka 1998; Boley et al. 2007) that accounts for the rotational and vibrational degrees of freedom of molecular hydrogen, and for the different chemical states of hydrogen and helium. We assume that ortho- and para-hydrogen are in equilibrium.

For the dust and gas opacity we use the parametrization by Bell & Lin (1994), $\kappa(\rho, T) = \kappa_0 \rho^a T^b$, where κ_0, a, b are constants that depend on the species and the physical processes contributing to the opacity at each ρ and T . The opacity changes due to ice mantle evaporation and the sublimation of dust are taken into account, along with the opacity contributions from molecules and H^- ions.

For the N -body part of the simulation, exploring the long-term dynamical evolution of the stars formed by fragmentation of the outer disc (from ~ 20 to 200 kyr), we use a fourth-order Hermite integration scheme (Makino & Aarseth 1992), with a conservative time-step criterion so that energy is conserved to better than one part in 10^8 (Hubber & Whitworth 2005).

3 DISC INITIAL CONDITIONS

Only a few extended massive discs have been observed around Sun-like stars (e.g. Eisner et al. 2005, 2008; Rodríguez et al. 2005; Eisner & Carpenter 2006). However, we suggest that this is because the outer parts of such discs are rapidly dissipated by gravitational fragmentation – rather than because they seldom form in the first place. Indeed, it seems that the formation of such discs is inevitable.

For example, a $1.4 M_{\odot}$ pre-stellar core with ratio of rotational to gravitational energy $\beta \equiv \mathcal{R}/|\Omega|$ will – if it collapses monolithically – form a protostellar disc with outer radius $R_{\text{DISC}} \sim 400 \text{ au}$ ($\beta/0.01$). Since the observations of Goodman et al. (1993) indicate that many pre-stellar cores have $\beta \sim 0.02$, the formation of extended discs should be rather common.

Alternatively, if an existing $0.7 M_{\odot}$ protostar attempts to assimilate matter with specific angular momentum h , this matter is initially parked in an orbit at $R_{\text{ORBIT}} \sim 400 \text{ au}$ ($h/5 \times 10^{20} \text{ cm}^2 \text{ s}^{-1}$)². The quantum of specific angular momentum used to normalize this relation is rather modest by protostellar standards, as can be seen by expressing it in terms of a lever-arm in parsecs and a velocity in kilometres per second, viz. $5 \times 10^{20} \text{ cm}^2 \text{ s}^{-1} \equiv (0.02 \text{ pc}) \times (0.1 \text{ km s}^{-1})$.

Previous simulations (Stamatellos et al. 2007b) suggest that the outer parts of massive extended discs fragment on a dynamical time-scale ($\lesssim 3 \text{ kyr}$), so they are indeed very short lived.

We shall assume a star–disc system (hereafter the *ur-system*), in which the central primary star (hereafter the *ur-star*) has initial mass $M_1 = 0.7 M_{\odot}$. Initially the disc (hereafter the *ur-disc*) has mass

$M_D = 0.7 M_\odot$, inner radius $R_{\text{IN}} = 40$ au, outer radius $R_{\text{OUT}} = 400$ au, surface density

$$\Sigma_0(R) = \frac{0.014 M_\odot}{\text{au}^2} \left(\frac{R}{\text{au}} \right)^{-7/4}, \quad (4)$$

temperature

$$T_0(R) = 250 \text{ K} \left(\frac{R}{\text{au}} \right)^{-1/2} + 10 \text{ K}, \quad (5)$$

and hence approximately uniform initial Toomre parameter $Q \sim 0.9$. Thus the disc is at the outset marginally gravitationally unstable. (The *ur*- prefix is used solely because it otherwise becomes difficult later on to discuss unambiguously the smaller discs that attend newly formed BDs, the orbital parameters of BD/BD binaries and so forth.) We have designed a disc with $Q < 1$ over a wide range of radii, because we are wanting to establish which parts of the disc can, and which cannot, fragment because they obey, or violate, the Gammie criterion.

The radiation of the ur-star is taken into account by invoking a background blackbody radiation field with temperature $T_0(R)$. In effect, this means that, if the material in the disc is heated by compression and/or viscous dissipation, it can only cool radiatively if it is warmer than $T_0(R)$ given by equation (5).

4 SIMULATIONS: OVERVIEW

We perform 12 simulations: 10 using 150 000 particles, one with 250 000 and one with 400 000 (the last two to check convergence). The minimum resolvable mass (corresponding to 100 SPH particles) is $\lesssim 0.5 M_J$, and therefore the Jeans condition is obeyed at all times.

All of the simulations start with the same ur-system (i.e. the same ur-disc and ur-star parameters). The only difference (apart from the number of particles in the last two simulations) is the random seed used to construct each ur-disc. Thus the Poisson density fluctuations are different in each simulation. This allows us to study the statistical properties of the stars produced.

Because the ur-discs are Toomre unstable, spiral arms form and sweep up material into dense condensations. Within a few thousand years, between five and 11 stars have condensed out of the disc. In all 12 simulations a total of 96 stars are formed. 3 per cent are PMs, 67 per cent are BDs and the rest are low-mass HBs (with masses up to $\sim 200 M_J \equiv 0.2 M_\odot$). (Hereafter BD statistics will include PMs, unless otherwise stated.)

Stars initially condense out of the ur-disc where $Q < 1$ and $t_{\text{COOL}} < 0.5 t_{\text{ORB}}$, i.e. typically at distances $R \gtrsim 100$ au from the central star. HBs generally form closest to the ur-star, and PMs form furthest from the ur-star. There are three factors producing this trend of lower mass stars forming further out in the ur-disc: (i) stars condensing out at small R condense out earlier, so they then have longer to accrete; (ii) the ambient density at small R is higher, so there is more matter to accrete and (iii) the most massive stars tend to migrate inwards, so they get to mop up the inner parts of the ur-disc where no stars have condensed out.

With between five and 11 stars formed in each ur-disc, initially between ~ 60 and ~ 400 au, interactions between the stars are frequent. During two-body interactions, binary systems can be formed if there is sufficient dissipation (e.g. due to the small accretion discs which normally attend the individual stars). In three-body interactions, the lowest mass star is often ejected into the field, and therefore stops accreting altogether. 55 per cent of the stars formed end up being ejected into the field. Most of the stars below the

H-burning limit, and all the stars below the D-burning limit are ejected into the field.

Most are ejected as single stars, but some are ejected as components of binary systems. These binary systems comprise BD/BD pairings, BD/HB pairings and even one BD/PM pairing; there are both wide and close systems.

Ejected BDs frequently retain accretion discs with masses on the order of a few Jupiter masses. Hence they can sustain accretion and outflows as observed (Jayawardhana, Mohanty & Basri 2003; Mohanty, Jayawardhana & Basri 2005; Muzerolle et al. 2005; Whelan et al. 2005).

The final outcome typically has a low-mass HB orbiting the ur-star at close distance ($R \lesssim 10$ to 20 au), a low-mass HB in a wider orbit, and a couple of BDs or a BD/BD binary orbiting at large distance ($R \gtrsim 100$ to 200 au). All the other stars have been ejected into the field.

In Fig. 1 we present column density images of the ur-disc, every 500 yr, for one of the simulations. In this simulation seven stars form: four BDs and three low-mass HBs. At the end of the simulation (i.e. after the hydrodynamic simulation *and* the N -body simulation, at 200 kyr), only three stars remain bound to the ur-star: a low-mass HB orbiting close to the ur-star ($R \sim 10$ au), and a binary comprising a BD and a low-mass HB, orbiting at $R \sim 7700$ au.

Fig. 2 shows the Toomre parameter Q and the ratio of the cooling time to the orbital time $t_{\text{COOL}}/t_{\text{ORB}}$ (both azimuthally averaged), every 1 kyr from 0 to 6 kyr. Initially the ur-disc is marginally unstable (blue line), and outside 100 au the cooling time is favourable for fragmentation (i.e. $t_{\text{COOL}} < 0.5 t_{\text{ORB}}$). Hence the ur-disc fragments here. As time progresses the region where $Q < 1$ moves farther away from the ur-star as the gas in the inner regions is used up.

In the two simulations with higher resolution, the growth of gravitational instabilities, and the properties of the stars formed as a result of these instabilities, follows the same patterns as in the simulations with lower resolution. The variance is the same as between two simulations performed with the same resolution, and is attributable to the different seed noise in the different simulations (due to random positioning of the particles) and the chaotic, non-linear nature of gravitational instability. Thus, the simulations appear to be converged, in a statistical sense.

In the following sections we describe in detail the results of the simulations, focusing on the statistical properties of the stars formed, and compare them with the observed properties of BDs and low-mass HBs.

5 STATISTICAL PROPERTIES OF THE LOW-MASS STARS PRODUCED BY DISC FRAGMENTATION

5.1 Formation time

The ur-discs start fragmenting after 2 kyr, which corresponds to about one quarter of an outer rotation period (1 ORP = 8 kyr; see Fig. 3). Stars condense out on a dynamical time-scale. Hence star formation occurs faster in the inner ur-disc, but even at the edge of the ur-disc it is virtually over by 1 ORP. The stars which form first, in the inner ur-disc, have more time to accrete, and more material to accrete, and hence they tend to end up as HBs, with masses up to $\sim 200 M_J$ (see Fig. 3). Lower mass stars (i.e. BDs and PMs) tend to form at later times and at larger distances from the ur-star.

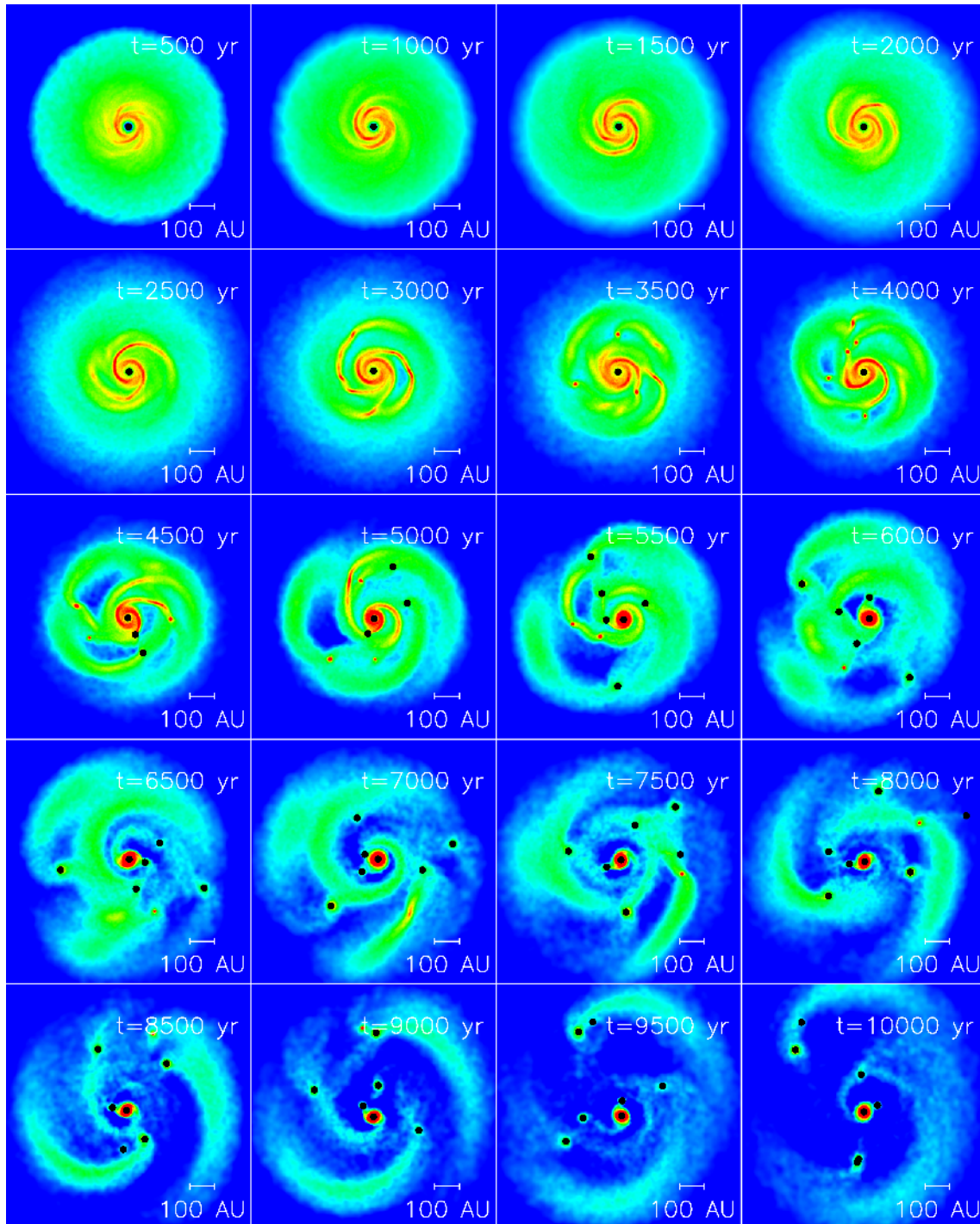


Figure 1. Radiative hydrodynamic simulation of the evolution of a $0.7\text{-}M_{\odot}$ ur-disc around a $0.7\text{-}M_{\odot}$ ur-star. Snapshots of the logarithm of the column density are presented from 0.5 to 10 kyr, every 0.5 kyr (as marked on each graph). Such ur-discs are gravitationally unstable and they cool efficiently. Hence they quickly fragment to form BDs and low-mass HBs. This particular simulation produces four BDs and three low-mass HBs. After 200 kyr, four of these stars have been ejected into the field.

5.2 Mass distribution

The mass distribution of the objects produced by disc fragmentation is shown in Fig. 4. ~ 70 per cent of the stars produced have masses below the H-burning limit, and ~ 3 per cent of these have masses below the D-burning limit. The mass distribution peaks around 30 to 40 M_{J} . It decreases smoothly towards higher masses,

roughly as $dN/dM \propto M^{-\alpha}$, with $\alpha \simeq 1.4$. There is no significant discontinuity across the H-burning limit at $\sim 80 M_{\text{J}}$. The mass distribution drops precipitously towards lower masses, reflecting that the minimum mass for star formation is $M_{\text{MIN}} \sim 5 M_{\text{J}}$. The small number of stars that end up below the D-burning limit are the ones that are ejected from the ur-disc by a three-body interaction, almost as soon as they have formed.

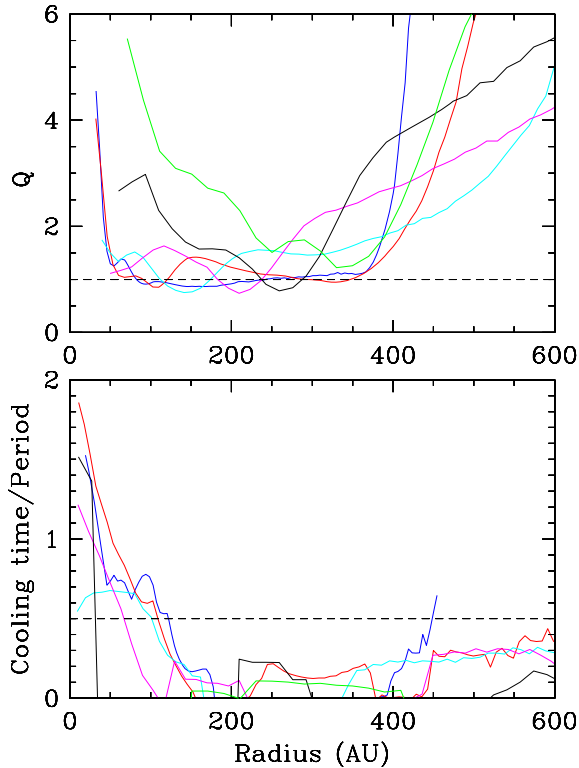


Figure 2. The Toomre parameter Q and the ratio of the cooling time to the orbital period $t_{\text{COOL}}/t_{\text{ORB}}$ (both azimuthally averaged) are plotted against distance from the ur-star, every 1 kyr from 0 to 6 kyr (blue, red, cyan, magenta, black, green).

We emphasize that the mass function presented in Fig. 4 represents stars formed by fragmentation of a particular ur-system (i.e. an ur-disc with mass $M_{\text{DISC}} = 0.7 M_{\odot}$, radius $R_{\text{DISC}} = 400$ au etc. in orbit round a ur-star with mass $M_1 = 0.7 M_{\odot}$). Therefore, it cannot be compared meaningfully with the overall stellar IMF. Rather it will be necessary first to repeat the numerical experiment reported here for many different ur-systems (i.e. different combinations of M_{DISC} , R_{DISC} and M_1 , etc.), and then to convolve the results with the appropriate distributions of M_{DISC} , R_{DISC} and M_1 , before comparing with the observed stellar IMF. A Monte Carlo experiment addressing this aspect of the problem is in progress (Attwood et al., in preparation).

5.3 Radial distribution and the brown dwarf desert

Fig. 5 shows the radial distribution of the stars formed by disc fragmentation, i.e. the distance R from the ur-star. Radial distributions are shown for all stars, and then separately for HBs and BDs, (i) at the moment of formation (~ 5 kyr; left), (ii) at the end of the SPH simulation (~ 20 kyr; centre) and (iii) at the end of the N -body simulation (200 kyr; right). Stars are categorized as HBs or BDs on the basis of their final masses; here the BD category includes the PMs.

The most likely location at which stars form is between 100 and 200 au from the ur-star (Fig. 5; left). This is the combined effect of the two criteria for disc fragmentation discussed in Section 1.

Close to the central primary star ($R \lesssim 60$ au), there is ample mass for fragmentation, so the Toomre criterion is satisfied ($Q \leq 1$). However, the cooling time is high compared with the orbital period, and hence stars cannot condense out fast enough and they are quickly

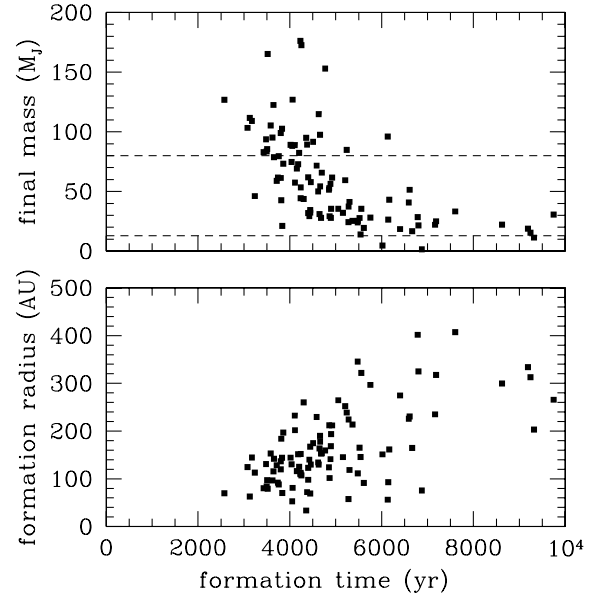


Figure 3. The final mass and formation radius of the stars formed by disc fragmentation plotted against formation time (top and bottom, respectively). Stars form between 2 and 10 kyr. In general, more massive stars form earlier and closer to the ur-star, whereas lower mass stars form later and farther from the ur-star.

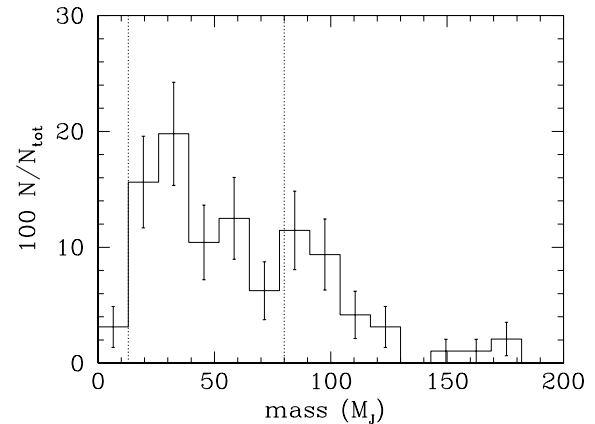


Figure 4. Mass spectrum of the stars produced by disc fragmentation. Most of the stars are BDs (70 per cent); the rest are low-mass HBs. The perpendicular dotted lines correspond to the D-burning limit ($\sim 13 M_J$) and the H-burning limit ($\sim 80 M_J$). The mass used for the histogram is the mass that the star has at the end of the SPH simulation. Most of the stars are still accreting gas, so their final masses are likely to increase by a few per cent. The error bars correspond to the Poisson statistical noise.

sheared apart. This minimum radius for fragmentation agrees well both with analytical predictions (Rafikov 2005; Whitworth & Stamatellos 2006), and with previous numerical simulations (see also Stamatellos et al. 2007b; Stamatellos & Whitworth 2008).

Conversely, far from the ur-star ($R > 300$ au), the cooling time is quite low, but there is only just enough mass for the disc to be Toomre unstable ($Q \sim 1$), and so fragmentation is sluggish.

At locations between $R \sim 100$ and ~ 200 au the conditions are just right for vigorous fragmentation to occur.

In the lower panels of Fig. 5 (left), we show separately the formation locations of HBs and BDs. Stars forming close to the ur-star

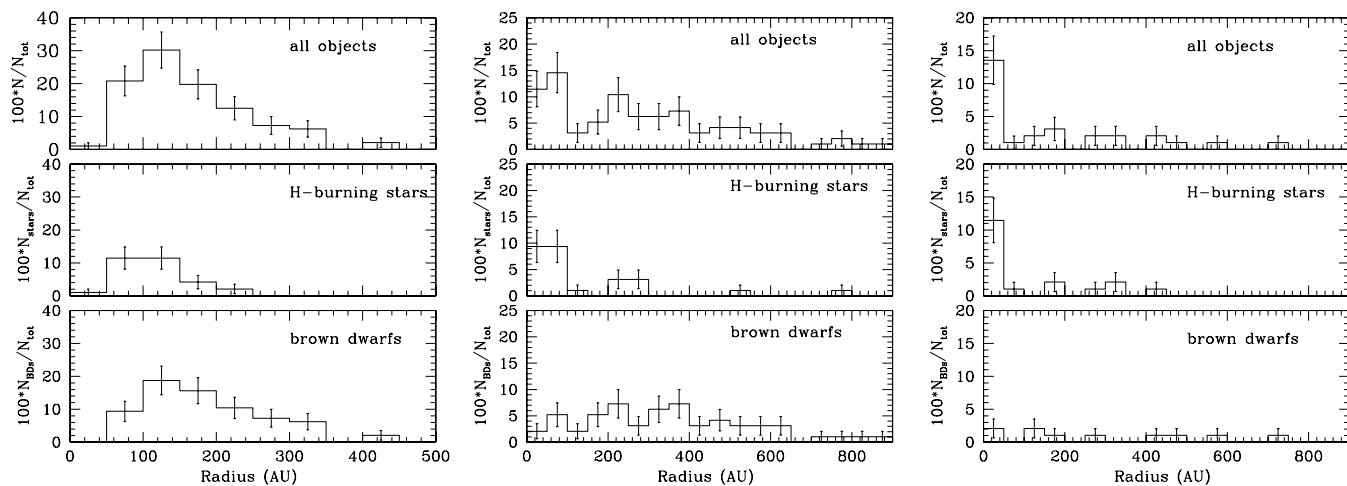


Figure 5. Radial distribution of the stars: (i) at the moment of formation (~ 5 kyr; left), (ii) at the end time of the SPH simulation (~ 20 kyr; centre) and (iii) at the end of the N -body simulation (200 kyr). The radial distribution is plotted for all stars (top), for the HBs alone (middle) and for the BDs alone (bottom).

generally accrete more gas and so their masses tend to increase above the H-burning limit.

The initial radial distribution quickly changes due to dynamical interactions between the newly formed stars. In each disc between five and 11 stars form between 60 and 400 au. Therefore, the probability for interactions is high. In Fig. 5 (centre) we present the radial distribution of the stars at the end of the SPH simulation at ~ 20 kyr. The HBs are mostly within 100 au of the ur-star, whereas the BDs are mostly outside 100 au.

The radial distribution has changed even more by the end of the N -body evolution, after 200 kyr (Fig. 5; right). Most HBs have remained bound to the ur-star (half at close distances, ~ 10 au and the rest on wider orbits of a few hundred au). On the other hand, most of the BDs have been ejected, and those that remain bound to the ur-star have wide orbits of a few hundred au.

This is also seen in Fig. 6, where the object final mass is plotted against the radius at formation (top), the radius at the end of the SPH simulation (20 kyr; middle) and the radius at the end of the N -body simulation (200 kyr; bottom). Both HBs and BDs form over a wide range of radii, but after the system has evolved for 200 kyr there are 13 HBs orbiting within 60 au of the ur-star, and only one BD. The HBs, being more massive, tend to form at smaller radii, and during dynamical three-body interactions the more massive stars tend to become more tightly bound.

This phenomenology provides a natural explanation for the brown dwarf desert, i.e. the lack of BDs as close companions to Sun-like stars ($R \lesssim 5$ au; Marcy & Butler 2000) in contrast with the relatively high frequency of both HBs and planets at these radii. First, stars with masses below the H-burning limit only condense out of the ur-disc at large radii ($\gtrsim 100$ au) – as predicted analytically by Whitworth & Stamatellos (2006). Secondly, such stars are only likely to stay below the H-burning limit if they remain at large radius or are ejected from the ur-disc. Thirdly, the interactions which occur between stars formed in the ur-disc tend to scatter the more massive ones inwards and the less massive ones outwards. Consequently the more massive stars tend to end up in the inner parts of the ur-disc where there is still gas to be accreted, and hence they tend to grow even more massive until they exceed the H-burning limit.

At the end of our simulations, only one of the 12 ur-stars has a close (< 30 au) brown dwarf companion, whereas there are 12 low-mass HBs in the same radial interval. Hence, it is ~ 12 times

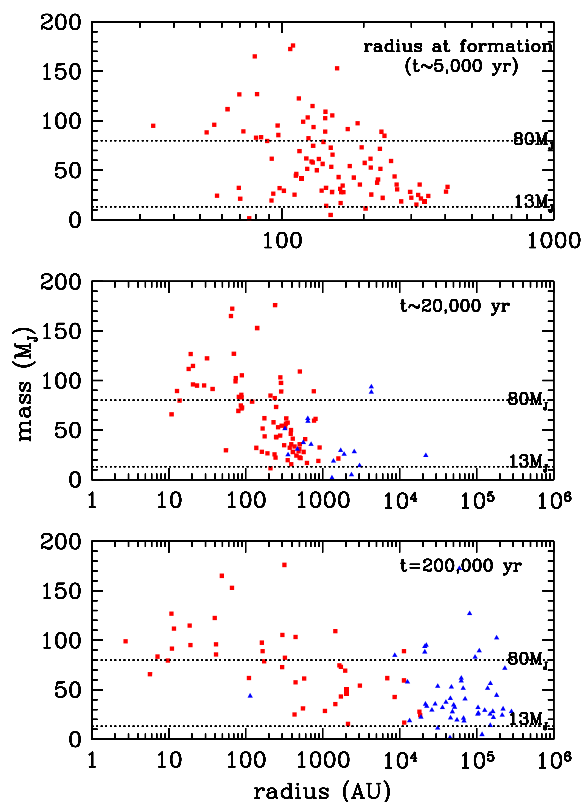


Figure 6. The origin of the brown dwarf desert. The formation radius (top), the radius at $t \sim 20$ kyr (middle) and the radius at $t = 200$ kyr, are plotted against the final stellar mass. HBs are scattered towards the ur-star, whereas BDs are ejected or migrate towards wider orbits. Hence, the region close to the ur-star is exclusively populated by low-mass HBs. The blue triangles correspond to objects that are ultimately not bound to the ur-star (ejected or about to be ejected from the system).

more likely for the close companion of a Sun-like star to be an HB, rather than a BD. This is comparable with observations, which suggest that < 0.5 per cent of Sun-like stars have BD companions within ~ 5 au (e.g. Marcy & Butler 2000; Udry, Mayor & Queloz 2003), or < 2 per cent within ~ 8 au (e.g. in the Hyades cluster;

Guenther et al. 2005). This fraction rises to ~ 13 per cent for HB companions (Duquennoy & Mayor 1991), i.e. HB companions are between seven and 25 times more frequent than BD companions.

In fact, at the end of our simulations only four out of 24 (~ 17 per cent) of the stars within ~ 400 au of the ur-star are BDs, suggesting that the brown dwarf desert extends to a wider region around Sun-like stars. This is consistent with the results of the *Gemini* Deep Planet Survey that found a very low probability of BDs [with $m < 40 M_J$ in the region 25–250 au (~ 1.9 per cent; Lafrenière et al. 2007)]. Hence, systems like 1RXSJ160929.1–210524, a PM with mass $8_{-1}^{+4} M_J$ orbiting a star with $0.85_{-0.1}^{+0.2} M_{\odot}$ at ~ 330 au (Lafrenière, Jayawardhana & van Kerkwijk 2008) can be explained with this model; however, such systems should be rare.

In contrast, BDs dominate the region from ~ 400 to $\sim 10\,000$ au; 19 out of 22 (~ 86 per cent) of the stars at these large radii are BDs. Gizis et al. (2001) report that at separations $\gtrsim 1000$ au Sun-like stars have comparable numbers of brown dwarf and M dwarf companions.

Once again, we should not necessarily expect a detailed correspondence with the observations, because we have only studied a single ur-system (i.e. a single combination of M_{DISC} , R_{DISC} , M_1 etc.).

5.4 Orbital plane of the bound objects

Initially (at formation time, ~ 5 kyr) the orbits of the stars formed in the ur-disc are almost coplanar with the ur-disc; their orbital planes all lie within 5° of the ur-disc plane (Fig. 7, top). However, due

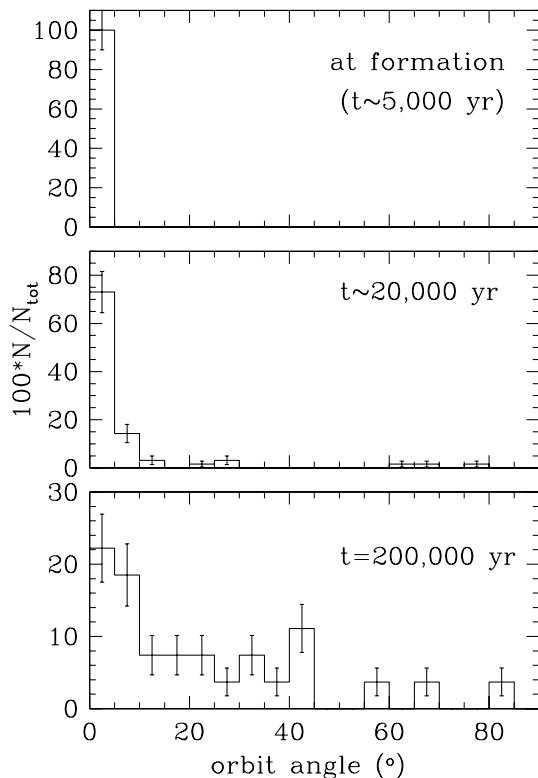


Figure 7. The distribution of inclination angles between the orbital planes of the stars and the orbital plane of the ur-disc, at formation ($t \sim 5$ kyr; top), at $t \sim 20$ kyr (middle) and at $t = 200$ kyr (bottom). The stars form very close to the ur-disc mid-plane (within $\pm 4^\circ$) but due to three-body interactions many of them acquire inclined orbits. Coplanarity is not a characteristic of disc fragmentation.

to three-body interactions the stars start to acquire inclined orbits. By ~ 20 kyr only ~ 70 per cent of the orbital planes lie within 5° of the ur-disc plane, and by ~ 200 yr this percentage has dropped to ~ 22 per cent (Fig. 7, middle and bottom). We expect that in a realistic asymmetric disc, still accreting from its natal cloud, these percentages will be even smaller.

The inclination of the orbital plane does not appear to depend on the mass of the star, or its distance from the ur-star. Consequently, coplanarity in observed multiple systems, or the absence of it, cannot confirm or rule out formation by disc fragmentation.

5.5 Disc properties of low-mass objects formed by disc fragmentation

When stars condense out of the ur-disc, they are normally attended by their own individual accretion discs, but some of these individual discs are subsequently stripped by dynamical interactions. At the end of the SPH simulation (~ 20 kyr), ~ 70 per cent of the stars still have individual accretion discs. In addition, some of the binary systems have circumbinary discs.

These percentages are comparable with, but somewhat higher than, those reported in the literature. Jayawardhana et al. (2003) found a disc fraction of 40 to 60 per cent in a mixed sample from Chamaeleon I, IC 348, Taurus and U Sco, using *JHKL* photometry. Luhman et al. (2005b), using *Spitzer* NIR (near-infrared) observations, found a disc fraction of 42 ± 13 per cent for IC 348 and 45 ± 7 per cent for Chamaeleon I. However, these observed statistics correspond to stars in the fields of these clusters (i.e. stars which, if they have been formed by fragmentation of an ur-disc, have since been ejected) and so we expect their disc frequency to be somewhat reduced.

Of the 13 systems (11 singles and two binaries) ejected by the end of our SPH simulations at ~ 20 kyr, only one of the singles, but both the binaries, retain discs. Thereafter, the simulation switches to an N -body code, and so we cannot say anything quantitative about how the disc statistics subsequently evolve. However, since there are many stars with discs orbiting at very large distances from the ur-star – for example, at the end of the SPH simulations, there are 16 systems, including two binaries, orbiting at $R \gtrsim 500$ au – we should expect many of these to be liberated from the ur-star by the tides of passing stars, and to retain their discs (e.g. Whitworth & Stamatellos 2006; Goodwin & Whitworth 2007). Thus we infer that young BDs in the field should have a significant disc fraction, and that young BDs orbiting Sun-like stars at large radius should have an even higher disc fraction.

The masses and radii of individual discs are plotted against the masses of their host stars in Fig. 8. The disc masses are generally $\lesssim 10 M_J$, but there are a couple of discs with higher masses (a few tens of M_J). There seems to be no correlation between the disc masses and the star masses. The disc radii range up to 100 au, but most of them are $\lesssim 70$ au. Again there seems to be no correlation between disc radius and star mass.

The individual discs around BDs and HBs are statistically indistinguishable. The distributions of mass and radius for discs around BDs are shown in Fig. 9. Most BD discs (~ 80 per cent) have masses below $\sim 5 M_J$, but the mass can be as high as $\sim 15 M_J$ (Fig. 9, top). Most BD discs have radii $\lesssim 60$ au, but the radius can be as high as 100 au (Fig. 9, bottom). These disc masses and radii are consistent with observations, which show discs to be very common around BDs (Klein et al. 2003; Luhman 2004; Luhman et al. 2005c; Scholz, Jayawardhana & Wood 2006; Guieu et al. 2007; Riaz & Gizis 2007, 2008), even around very low-mass ones (e.g. Luhman et al. 2005a).

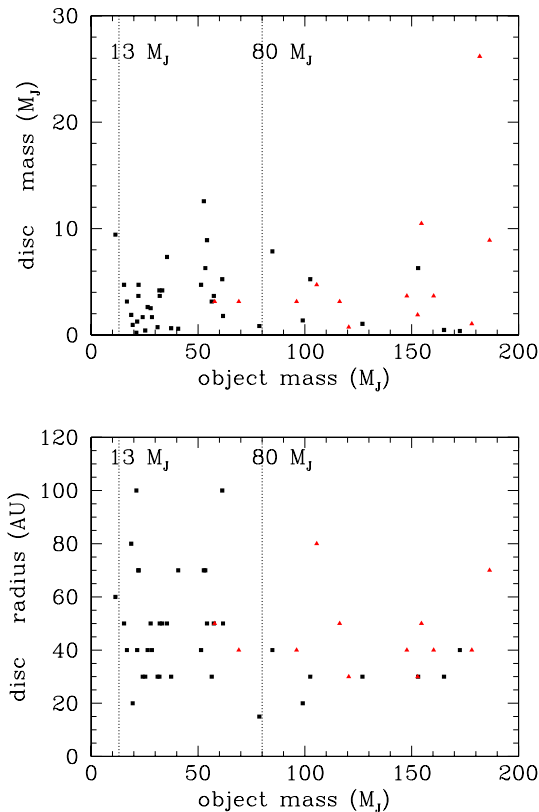


Figure 8. Disc masses (top) and radii (bottom) plotted against the masses of the host stars. The red triangles correspond to circumbinary discs.

The BD discs are massive enough to make the formation of rocky planets with masses up to $5 M_{\oplus}$ around BDs a plausible scenario, at least around some of them (Payne & Lodato 2007).

5.6 Low-mass binary properties

Here we discuss the statistical properties of the binary systems that exist at the end of the simulations. We confine the discussion to binaries in which both components are stars that have condensed out of the disc, and we refer to these as low-mass binaries. There are also binary systems and higher multiples in which one of the component is the ur-star; we do not discuss these here.

Our simulations produce 13 low-mass binaries, of which four comprise two low-mass HBs, four comprise a low-mass HB and a BD, four comprise two BDs and one comprises a BD and a PM. The main properties of these binaries are recorded in Table 2. In total, 27 per cent of the stars that form end up in binary systems, corresponding to a binary fraction of 16 per cent. This is comparable with the low-mass binary fraction in Taurus–Auriga ($\lesssim 20$ per cent; Kraus, White & Hillenbrand 2006), Chamaeleon I (11^{+9}_{-6} per cent; Ahmic et al. 2007) and the field (e.g. 15 ± 5 per cent; Gizis et al. 2003). However, these are optical surveys and they are not able to detect tight binaries with separation of a few au. If we consider only the two wide binaries then the binary fraction we estimate is ~ 2.5 per cent, which is smaller than observed. Very tight binaries can be probed by radial velocity surveys (Joergens 2006a, 2008; Kurosawa, Harries & Littlefair 2006; Maxted et al. 2008). These surveys find a low-mass tight-binary fraction of 10–30 per cent which is consistent with our model.

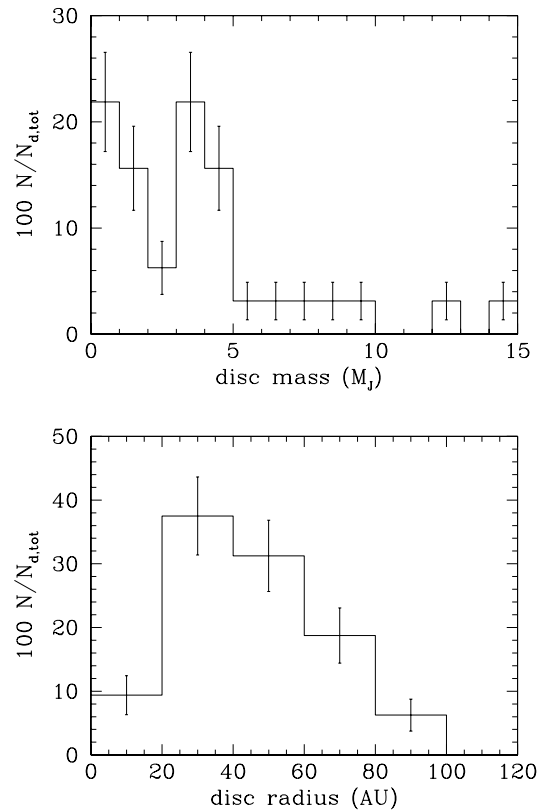


Figure 9. Mass (top) and size (bottom) distribution of the discs around brown dwarfs formed by fragmentation of the ur-disc.

Table 2. Properties of low-mass binaries (i.e. those in which both components have condensed out of the disc): m_p , the primary mass; m_s , the secondary mass; $q = m_s/m_p$, the mass ratio; a_{BIN} , the semi-major axis of the low-mass binary orbit; e_{BIN} , the eccentricity of the low-mass binary orbit; a , the semimajor axis of the orbit of the low-mass binary around the ur-star (in those cases where the low-mass binary remains bound to the ur-star, otherwise blank). The binaries are grouped into four categories, according as the components are (i) both HBs, (ii) an HB and a BD, (iii) both BDs and (iv) a BD and a PM.

m_p (M_J)	m_s (M_J)	q	a_{BIN} (au)	e_{BIN}	a (au)
96	86	0.90	0.3	0.4	20
98	89	0.91	1.4	0.5	140
176	82	0.47	1.5	0.8	230
88	83	0.94	0.3	0.7	–
89	59	0.66	1.0	0.9	7700
102	44	0.43	0.3	0.8	–
109	35	0.33	0.6	0.8	800
105	73	0.70	0.5	0.3	200
50	46	0.92	0.6	0.5	1500
28	24	0.86	235	0.7	4000
62	59	0.95	0.6	0.9	–
73	43	0.59	1.3	0.7	1350
53	11	0.21	112	0.6	–

11 of the 13 low-mass binaries have semimajor axes $a_{\text{BIN}} < 2$ au. Thus we predict that close low-mass binaries should outnumber wide ones, and this seems to be what is observed (e.g. Burgasser et al. 2007). In Fig. 10 (top) we plot the projected separation

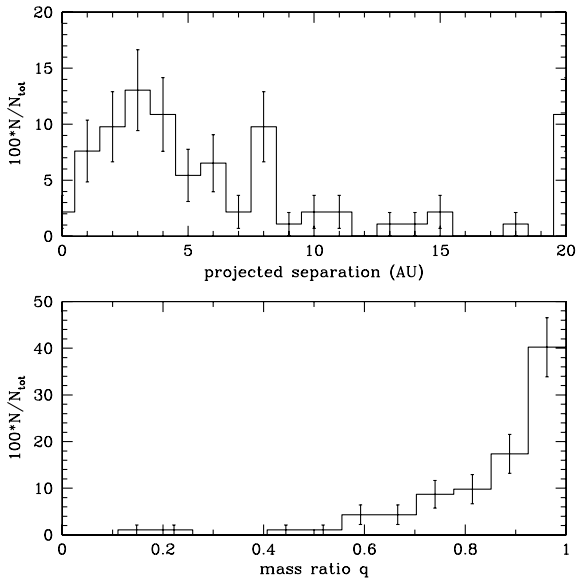


Figure 10. The observed properties of very low-mass binaries: projected separation (top) and mass ratio (bottom) distributions (data are taken from <http://www.vlmbinaries.org>; last updated on 2008 February 4).

distribution for the very low mass binaries from the <http://www.vlmbinaries.org> dataset. In this dataset only ~ 10 per cent of the binaries have separations > 20 au, which is similar to the predictions of our model (2/13 binaries, i.e. 15 per cent). We note that in Table 2 we quote the semimajor axis of the binary, whereas Fig. 10 refers to the projected separation, which for eccentric binaries is most often larger than semimajor axis. The two wide low-mass binaries – with $a_{\text{BIN}} = 112$ and 235 au – are the systems with the lowest total mass.

Four low-mass binaries, including one of the very wide systems, have become unbound from the ur-star. Therefore, the ejection mechanism does not militate against delivering wide low-mass binaries to the field. One of the unbound low-mass binaries comprises a BD and a PM; it is therefore quite similar to 2MASS 1207–3932 (Chauvin et al. 2004, 2005).

Amongst the nine low-mass binaries that remain bound to the ur-star, the semimajor axis a of the orbit around the ur-star tends to increase as the total mass of the low-mass binary decreases. Thus most of the low-mass binaries with an HB primary orbit the ur-star within 1000 au, whereas most of the low-mass binaries with a BD primary orbit the ur-star outside 1000 au.

All of the low-mass binaries have high eccentricities, as a result of the dynamical interactions which form them, and/or subsequent dynamical interactions with other stars that have condensed out of the ur-disc. The high eccentricities of the wide binaries should persist, but the high eccentricities of the closer binaries may be damped somewhat by tidal interaction between their attendant discs; these tidal interactions are not accounted for in our N -body simulations.

Most of the low-mass binaries (55 per cent) have components with similar masses ($q > 0.7$), in agreement with the observed properties of low-mass binaries (e.g. Burgasser et al. 2007; see Fig. 10).

25 (out of 67, i.e. 37 per cent) of the BDs formed in the ur-disc remain bound to the ur-star. The remaining 42 (out of 67, i.e. 63 per cent) are ejected. Of the 25 BDs that remain bound to the ur-star, 10 (40 per cent) are in low-mass binaries. In contrast, of the 42 BDs that become unbound from the ur-star, only five (12 per cent) are in low-mass binaries (one with an HB primary). Hence,

BDs that are companions to Sun-like stars are more likely to be in binaries (binary frequency 25 per cent) than BDs in the field (binary frequency 5 to 8 per cent). This trend is comparable to what is observed, although the observed binary frequencies are somewhat higher. Burgasser, Kirkpatrick & Lowrance (2005) report a binary fraction of 45^{+15}_{-13} per cent for BD companions to Sun-like stars, and a binary fraction of only 18^{+7}_{-4} per cent for BDs in the field.

5.7 Accretion

Newly formed stars continue to accrete material from the ur-disc. Stars forming closer to the ur-star tend to accrete more material than stars forming further away, first because there is more material in the inner parts of the ur-disc to accrete (particularly in the innermost part of the ur-disc, which is unable to fragment), and secondly because the more massive stars tend to migrate inwards. In our simulations, typical accretion rates are $\gtrsim 10^{-6} M_{\odot} \text{ yr}^{-1}$, which is high compared with the observed accretion rates on to brown dwarfs (typically $\lesssim 10^{-8} M_{\odot}$; e.g. Natta et al. 2004; Mohanty et al. 2005; Muzerolle et al. 2005; Herczeg & Hillenbrand 2008). However, the high accretion rates we record refer to an early, short-lived phase ($\lesssim 15$ kyr), and they are expected to decline significantly at later times.

The accretion rates often exhibit periodic modulations, during which the rate may increase by more than an order of magnitude. These modulations are partly due to high orbital eccentricity, and correspond to periastron passages within $R \sim 20$ to 50 au, occurring every few thousand years. There are also smaller modulations involving the components of close binaries as material is accreted on to them from a circumbinary disc. Finally, there are occasional episodic events when the accretion rate increases by up to an order of magnitude as a star passes through a spiral arm in the ur-disc or through the disc of another star.

In Fig. 11 we plot – for the simulation presented in Fig. 1 – the accretion rates on to the ur-star and on to the seven stars formed from the ur-disc. These plots are representative of the accretion rates on to stars in the other simulations. On the first plot, we present the accretion rate on to the ur-star (black line). The accretion rate initially increases, as the inner gap is filled in, and then remains approximately constant around $\dot{M}_1 \sim 5 \times 10^{-5} M_{\odot} \text{ yr}^{-1}$. The other star presented on the first plot (red line) is one which is ejected and so accretion is effectively terminated. There is actually a very low persistent accretion rate on to this star, because it retains a small accretion disc, but the rate is well below $10^{-8} M_{\odot} \text{ yr}^{-1}$.

On the second plot we present the accretion rates on to two stars which form at different times but eventually become a binary system with a circumbinary disc. The star which forms later, and at larger distance from the ur-star, initially accretes less material than the star which forms earlier, and closer to the ur-star. After the binary forms, the accretion rates on to the two stars become very similar.

On the last two plots, the accretion rates on to the other four stars are presented. Again it can be seen that the stars which form later tend to accrete less than the stars which form earlier. In some instances the difference exceeds an order of magnitude. The stars which experience persistently higher accretion rates tend to be the ones that form, and/or end up, closer to the ur-star.

6 AFTERMATH

6.1 The ur-star and its companions

The ur-discs dissipate on a dynamical time-scale, i.e. within a few thousand years. In Fig. 12 the mass of the remnant ur-disc is plotted

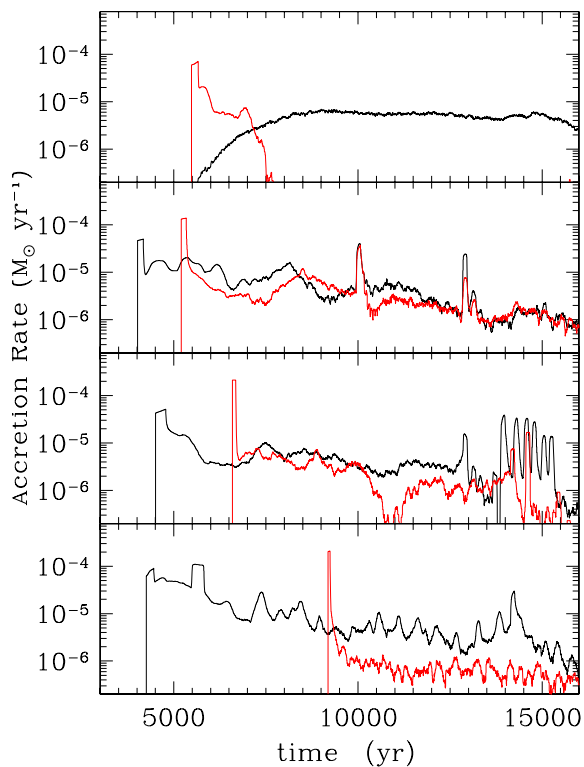


Figure 11. Accretion rates on to the stars forming in the simulation presented in Fig. 1. The first plot shows the accretion rate on to the ur-star (black line) and the accretion rate on to a star which is ejected (red line). The second plot shows the accretion rates on to two stars which eventually become a binary with a circumbinary disc. Stars which form earlier and/or closer to the ur-star (black lines on the last three plots) tend to accrete more than stars which form later and/or further away from the ur-star (red lines on the last three plots). The accretion rates show signs of periodic modulation (due to passing close to the ur-star and/or accretion from a circumbinary disc) and non-periodic modulation (when a star passes through a spiral arm or another star’s disc).

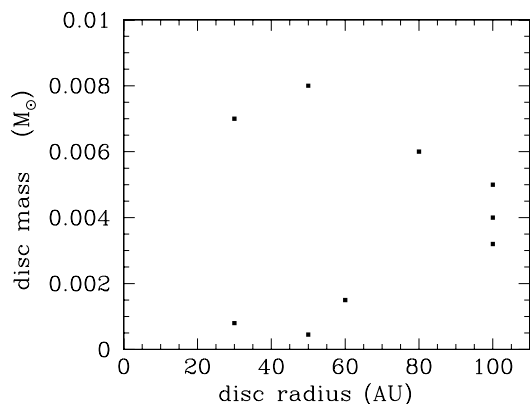


Figure 12. The masses and radii of the remnant ur-discs at the end of the SPH simulations, i.e. $t = 20$ kyr. Two cases fall outside this plot; they have $(M_{\text{DISC}}, R_{\text{DISC}}) \simeq (0.03 M_{\odot}, 200 \text{ au})$ and $(0.19 M_{\odot}, 150 \text{ au})$.

against its radius. By this stage, most of the ur-discs have masses $M_{\text{DISC}} \lesssim 0.01 M_{\odot}$, although one has $M_{\text{DISC}} \sim 0.2 M_{\odot}$. The ur-disc radii are all $R_{\text{DISC}} \lesssim 200 \text{ au}$. These ur-disc masses and radii are typical of the discs observed around Sun-like stars (e.g. Mundy, Looney & Lada 1995; Bally et al. 1998; Eisner et al. 2005, 2008; Williams, Andrews & Wilner 2005; Eisner & Carpenter 2006).

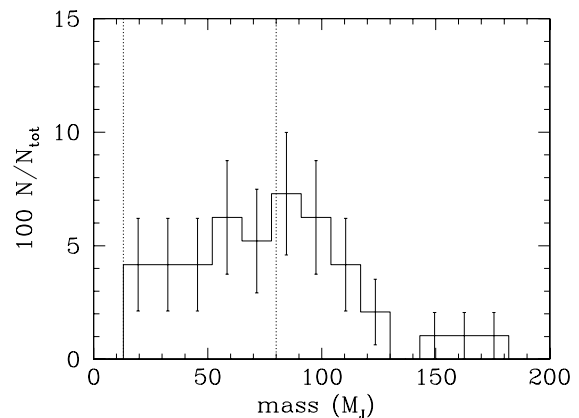


Figure 13. The mass distribution of stars which remain bound to the ur-star. There are almost equal numbers of HBs and BDs.

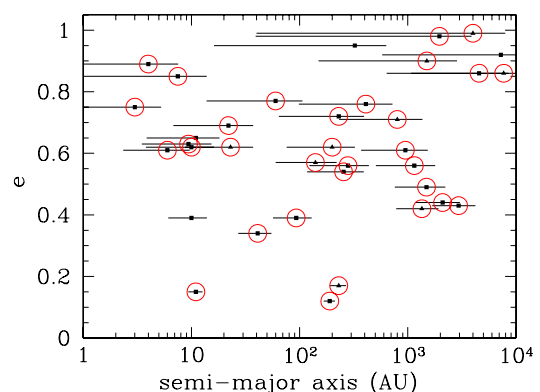


Figure 14. The orbital eccentricities and semimajor axes of stars which remain bound to the ur-star. The bars indicate the minimum and maximum extent of the orbit. The orbits are generally highly eccentric, as a result of dynamical interactions. The circles mark stars with discs, and the triangles correspond to binary systems.

In our simulations the ur-star ends up with one or two H-burning companions and one or two brown dwarf companions. The masses of the companions are almost equally distributed across the low-mass regime (see Fig. 13). One of the companions is in a relatively close orbit ($R \lesssim 20 \text{ au}$), and this one is almost always an H-burning star. The other two or three companions orbit much further out ($R \gtrsim 100 \text{ au}$), and often two of them are in a binary system.

The eccentricities of these wide companions are high, due to dynamical interactions with other stars (Fig. 14). Thus, although their semimajor axes are greater than 1000 au, due to their high eccentricity they pass within $\sim 100 \text{ au}$ of the ur-star with a periodicity between 10^4 and 10^7 yr , disrupting the remaining ur-disc and/or the orbits of any planets formed from the inner ur-disc (see Section 8).

6.2 The ejected population

More than half (55 per cent) of all the stars are ejected into the field. Nine (out of 29, i.e. ~ 30 per cent) of the HBs are ejected, and 45 (out of 67, i.e. ~ 67 per cent) of the BDs. The mass distribution of the ejected stars is shown in Fig. 15. Most of the objects ejected are low-mass BDs; there are also some PMs. Four binaries are ejected, of which one comprises two HBs, one comprises an HB and a BD, one comprises two BDs and one comprises a BD and a PM.

The velocity distribution of the ejected stars is shown in Fig. 16 (top). Most stars are ejected with low velocities ($\lesssim 3 \text{ km s}^{-1}$). HBs

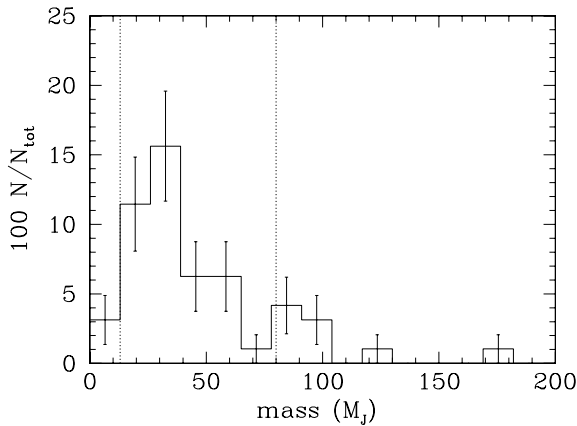


Figure 15. The mass distribution of the ejected stars. Most of them are low-mass BDs.

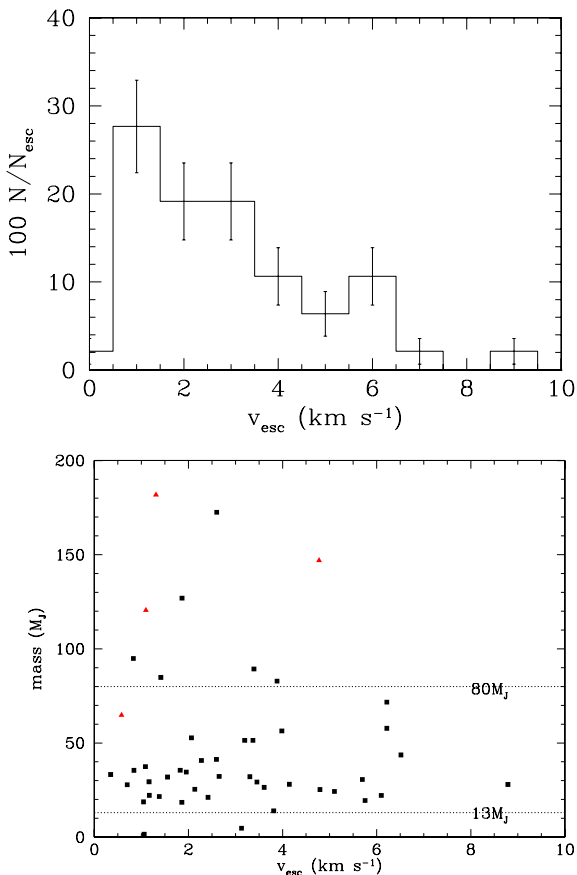


Figure 16. Top: the velocity distribution of the ejected stars; most stars are ejected with low velocities ($\lesssim 3 \text{ km s}^{-1}$). Bottom: the ejection velocities plotted against mass; HBs tend to be ejected with somewhat lower velocities.

tend to be ejected with somewhat lower velocities, but otherwise there is no strong dependence of the ejection velocity on the mass of the star (Fig. 16, bottom). A small percentage of the ejected stars in our simulations have very high velocities (cf. Umbreit et al. 2005), and the lack of such high velocities in observational surveys of BD kinematics, and the apparent absence of a diaspora of brown dwarfs around young star clusters, has often been used as an argument

against the ejection mechanism. However, in our simulations both BDs and HBs are ejected, and hence they should be roughly co-extensive (cf. Luhman 2004; Goodwin et al. 2005; Joergens 2006b). Moreover, the ejection velocities would be significantly lower if the ejection were treated fully with hydrodynamics, rather than invoking sinks and then switching to a N -body code.

7 RARE SYSTEMS FORMED BY DISC FRAGMENTATION

There are four types of system formed in our simulations that are rare but nevertheless have similarities with intriguing observed systems.

7.1 Free floating planetary-mass objects

Free floating PMs – i.e. single field stars with masses $< 13 M_J$ – have been observed in Orion (Lucas & Roche 2000), in the σ Orionis cluster (Zapatero Osorio et al. 2000) and in IC 348 (Najita, Tiede & Carr 2000). The simulations presented here show that such low-mass stars can form by disc fragmentation, and this is confirmed analytically by Whitworth & Stamatellos (2006). It is uncertain whether they can also form from the collapse of low-mass cores (e.g. Greaves 2005).

Three PMs form in our simulations, and all three of them are ejected into the field. Their masses remain below the D-burning limit because they are ejected from the disc very soon after formation. According to our simulations BDs should outnumber PMs by a factor of ~ 14 . Allowing for the fact that 35 per cent of the BDs remain bound to the ur-star but all PMs are ejected, BDs should outnumber PMs in the field by a factor of ~ 9 . However, we reiterate that these numbers are for a very specific ur-system.

7.2 Brown dwarf/planetary-mass binaries

One of the 13 low-mass binaries formed in our simulations has a $53 M_J$ BD primary and an $11 M_J$ PM secondary. This system has a semimajor axis of 110 au and an eccentricity of 0.6. The two components of the system formed independently by disc fragmentation, paired up in the disc and then were ejected as a binary into the field. This system is qualitatively similar to 2MASS 1207–3932 (Chauvin et al. 2004, 2005), a system with a $25 M_J$ BD primary orbited by a $5 M_J$ PM secondary, with a projected separation of 55 au. PMs are unlikely to be able to form by core accretion in BD discs (Lodato, Delgado-Donate & Clarke 2005; Payne & Lodato 2007). Lodato et al. (2005) suggest that 2MASS 1207–3932B may have formed by fragmentation of a disc around 2MASS 1207–3932A. We suggest that such systems form by pairing up of two components that form independently in a fragmenting disc, capture one another and then are ejected into the field as a binary.

7.3 Systems with non-coplanar discs

Four of the 58 circumstellar or circumbinary discs formed in our simulations are poorly aligned with the ur-disc (Fig. 17). This is because (a) stars do not form exactly on the mid-plane of the ur-disc, and (b) subsequently they experience impulsive perturbations due to passing stars that have formed in the disc. We presume that poorly aligned discs are even more common in real systems, i.e. asymmetric ur-discs forming in collapsing, fragmenting cores with lumpy material continuing to infall on to the ur-disc. The existence of poorly aligned discs is inferred from polarimetric observations

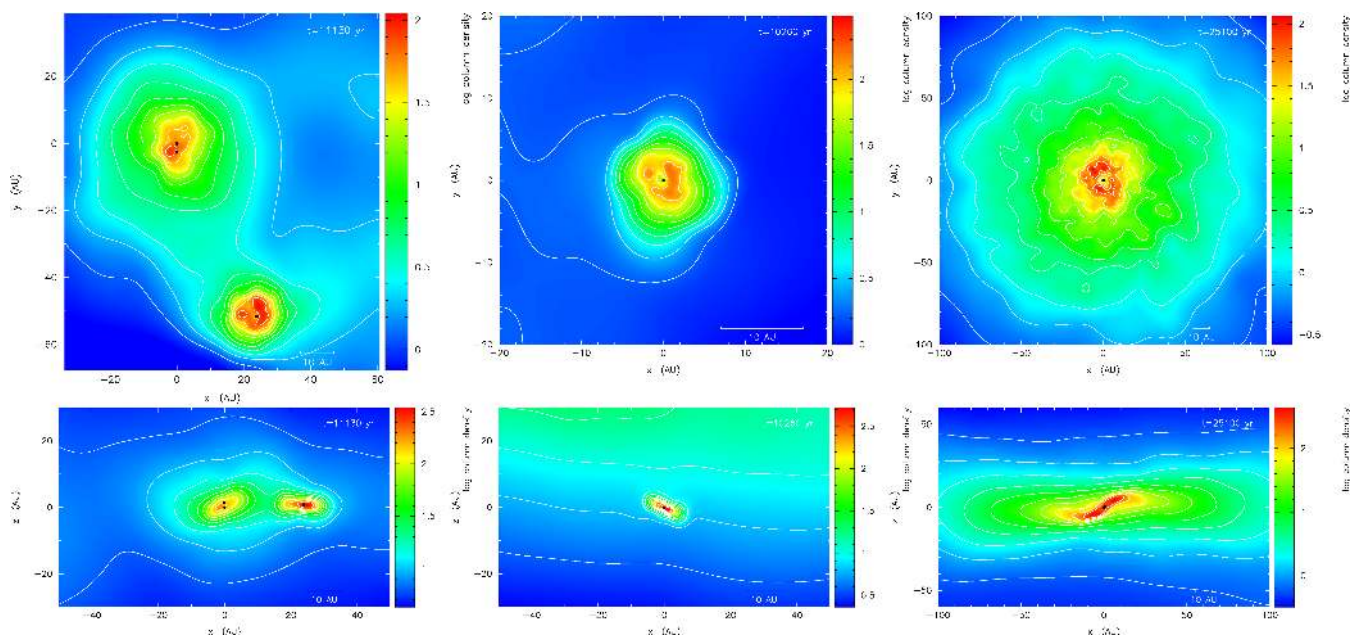


Figure 17. Rare systems produced by disc fragmentation. From left to right: (i) discs in a binary system which are aligned neither with each other nor with the ur-disc (the ur-disc is aligned with the $z = 0$ plane), (ii) disc that is not aligned with the ur-disc and (iii) a warped disc.

(Jensen et al. 2004; Monin, Ménard & Peretto 2006) and from non-parallel jets (e.g. Davis, Mundt & Eisloffel 1994).

7.4 Warped discs

One of the discs formed in our simulations is noticeably warped (see Fig. 17). The formation of such discs is a rare event, requiring a violent interaction between a star which is about to be ejected and a dense spiral arm. Warped discs have been observed (e.g. Heap et al. 2000; Quillen 2006).

8 IMPLICATIONS FOR PLANET FORMATION

Our simulations show that disc fragmentation can produce PMs, but the probability is low; for every PM formed, there are more than 30 BDs and/or HBs formed. The PMs form at large distances from the ur-star, and are then ejected before they have time to grow by accretion. If they were not ejected, they would grow in mass by accretion, and end up above the D-burning limit. Thus, it is very hard, if not impossible, for PMs to form in the outer reaches of massive extended ur-discs and then migrate inwards to a tight orbit around the ur-star.

Fragmentation is also unlikely to happen close to the ur-star (e.g. Matzner & Levin 2005; Rafikov 2005; Boley et al. 2006; Whitworth & Stamatellos 2006; Durisen et al. 2007; Stamatellos et al. 2007b; Cai et al. 2008; Stamatellos & Whitworth 2008).

Therefore, exoplanets (e.g. Udry & Santos 2007; *Extrasolar planets Encyclopaedia* at <http://exoplanet.eu>) probably have to form by the core accretion mechanism (e.g. Safronov 1969; Goldreich & Ward 1973; Pollack et al. 1996), at later stages during disc evolution. In fact even this may be rather hard in the ur-discs we have simulated here, although not necessarily in other discs. This is because each ur-disc we have simulated ends up with a low-mass star (usually an HB) on a close ($\lesssim 30$ au) eccentric orbit, and this is likely to inhibit planet formation in the inner disc (Thébaud, Marzari & Scholl 2006).

9 CONCLUSIONS

The fragmentation of massive, extended ur-discs produces stars which populate the low-mass end of the stellar IMF: low-mass HBs, BDs and PMs. Despite the fact that we have considered only a single ur-system, the predictions of the model compare well with observation. Simulations of different ur-systems (different ur-disc masses, radii, surface density profiles etc. and different ur-star masses) yield similar results (Stamatellos et al., in preparation), as do simulations in which we follow the formation of the ur-system from a collapsing turbulent pre-stellar core (Attwood et al., in preparation).

For the particular ur-system that we simulate (a $0.7 M_{\odot}$ 400 au disc in orbit about an $0.7 M_{\odot}$ star), we predict the following.

- (i) Each ur-disc fragments to form between five and 11 stars; 30 per cent are HBs, 67 per cent are BDs and 3 per cent are PMs.
- (ii) 55 per cent of the stars are ejected into the field (30 per cent of the HBs, 65 per cent of the BDs and 100 per cent of the PMs).
- (iii) The ur-star ends up with a close companion (usually an HB) and two or three wide companions (typically an HB and one or two BDs).
- (iv) These wide companions may include a low-mass binary system.
- (v) Within a few thousand years the ur-disc is reduced to $M_{\text{DISC}} \lesssim 0.01 M_{\odot}$ and $R_{\text{DISC}} \lesssim 100$ au.
- (vi) We hypothesize that there is a range of masses (say between ~ 0.05 and $\sim 0.2 M_{\odot}$) where – *proceeding to lower masses* – the balance gradually shifts *from* the majority of stars forming by turbulent fragmentation (as the ur-star presumably did) *to* the majority of stars forming as the result of fragmentation of discs around such stars (like the ur-disc).
- (vii) Only a small fraction (say 20 to 30 per cent) of the higher mass Sun-like stars (G, K and early M dwarfs) need to support disc fragmentation of the type we have modelled here to supply most of the low-mass HBs, BDs and PMs that are observed.
- (viii) Most stars initially condense out of the ur-disc between ~ 100 and ~ 200 au.

(ix) The stars forming closer to the ur-star tend to grow to become HBs, and may migrate inwards to much closer final orbits.

(x) The stars forming further out tend to migrate outwards and/or be ejected.

(xi) As a result there is a brown dwarf desert, i.e. a lack of brown dwarfs orbiting close to the ur-star; those brown dwarfs which are not ejected tend to end up orbiting out beyond ~ 200 au.

(xii) Because of dynamical interactions between stars, stellar orbits can end up quite eccentric and strongly inclined to the plane of the ur-disc.

(xiii) The majority of stars formed from the ur-disc have their own accretion discs, and some of these discs are retained during ejection; however, we expect BDs that remain bound to the ur-star to have a higher disc frequency than those which are ejected.

(xiv) Stars formed in the ur-disc frequently pair up to form low-mass binary systems. The low-mass binary frequency is ~ 16 per cent.

(xv) These binary systems are usually close, but can be wide; they tend to have eccentric orbits and large mass ratios (i.e. components of comparable mass); they include HB/HB pairs, HB/BD pairs, BD/BD pairs and BD/PM pairs.

(xvi) These binary systems can survive ejection; however, a BD that remains bound to the ur-star is three to five times more likely to be in a BD/BD binary system than a BD in the field.

(xvii) Ejection velocities are $\gtrsim 3 \text{ km s}^{-1}$, but these would probably be reduced if the hydrodynamics of ejection were modelled properly (i.e. not invoking sinks and not switching to an N -body code).

(xviii) Hot Jupiters are very unlikely to form by disc fragmentation. Moreover, in discs which fragment like the ones modelled here, formation of Hot Jupiters by core accretion may also be inhibited by the stellar companions that form on close eccentric orbits.

We conclude that disc fragmentation is a robust mechanism for the formation of BDs, as well as PMs and low-mass HBs. It explains successfully properties that are not satisfactorily explained by other formation mechanisms, for example the brown dwarf desert and the observed statistics of low-mass binary systems. We suggest that a large proportion of BDs and PMs may be formed by disc fragmentation.

ACKNOWLEDGMENTS

We would like to thank the referee for his helpful comments. The computations reported here were performed using the UK Astrophysical Fluids Facility (UKAFF). N -body simulations were done by a code originally developed by D. Hubber, who we thank for the support provided. We also thank Ken Rice, Aaron Boley and Viki Joergens for useful discussions/suggestions. We also gratefully acknowledge the support of an STFC rolling grant (PP/E000967/1) and a Marie Curie Research Training Network (MRTN-CT2006-035890).

REFERENCES

Ahmic M., Jayawardhana R., Brandeker A., Scholz A., van Kerkwijk M. H., Delgado-Donate E., Froebrich D., 2007, *ApJ*, 671, 2074
 Artymowicz P., Lubow S. H., 1994, *ApJ*, 421, 651
 Attwood R. E., Goodwin S. P., Whitworth A. P., 2007, *A&A*, 464, 447
 Bally J., Testi L., Sargent A., Carlstrom J., 1998, *AJ*, 116, 854
 Balsara D. S., 1995, *J. Comput. Phys.*, 121, 357
 Bate M. R., 1998, *ApJ*, 508, L95
 Bate M. R., Bonnell I. A., Bromm V., 2003, *MNRAS*, 339, 577

Bell K. R., Lin D. N. C., 1994, *ApJ*, 427, 987
 Black D. C., Bodenheimer P., 1975, *ApJ*, 199, 619
 Boley A. C., Mejía A. C., Durisen R. H., Cai K., Pickett M. K., D'Alessio P., 2006, *ApJ*, 651, 517
 Boley A. C., Hartquist T. W., Durisen R. H., Michael S., 2007, *ApJ*, 656, L89
 Boss A. P., Bodenheimer P., 1979, *ApJ*, 234, 289
 Boss A. P., Myhill E. A., 1992, *ApJS*, 83, 311
 Boss A. P., Fisher R. T., Klein R. I., McKee C. F., 2000, *ApJ*, 528, 325
 Boyd D. F. A., Whitworth A. P., 2005, *A&A*, 430, 1059
 Burgasser A. J., Kirkpatrick J. D., Lowrance P. J., 2005, *AJ*, 129, 2849
 Burgasser A. J., Reid I. N., Siegler N., Close L., Allen P., Lowrance P., Gizis J., 2007, in Reipurth B., Jewitt D., Keil K., eds, *Protostars and Planets V*. Univ. Arizona Press, Tucson, p. 427
 Cai K., Durisen R. H., Boley A. C., Pickett M. K., Mejía A. C., 2008, *ApJ*, 673, 1138
 Chauvin G., Lagrange A.-M., Dumas C., Zuckerman B., Mouillet D., Song I., Beuzit J.-L., Lowrance P., 2004, *A&A*, 425, L29
 Chauvin G., Lagrange A.-M., Dumas C., Zuckerman B., Mouillet D., Song I., Beuzit J.-L., Lowrance P., 2005, *A&A*, 438, L25
 Davis C. J., Mundt R., Eisloffel J., 1994, *ApJ*, 437, L55
 Duquennoy A., Mayor M., 1991, *A&A*, 248, 485
 Durisen R. H., Boss A. P., Mayer L., Nelson A. F., Quinn T., Rice W. K. M., 2007, in Reipurth B., Jewitt D., Keil K., eds, *Protostars and Planets V*. Univ. Arizona Press, Tucson, p. 607
 Eisner J. A., Carpenter J. M., 2006, *ApJ*, 641, 1162
 Eisner J. A., Hillenbrand L. A., Carpenter J. M., Wolf S., 2005, *ApJ*, 635, 396
 Eisner J. A., Plambeck R. L., Carpenter J. M., Corder S. A., Qi C., Wilner D., 2008, *ApJ*, 683, 304
 Gammie C. F., 2001, *ApJ*, 553, 174
 Gizis J. E., Kirkpatrick J. D., Burgasser A., Reid I. N., Monet D. G., Liebert J., Wilson J. C., 2001, *ApJ*, 551, L163
 Gizis J. E., Reid I. N., Knapp G. R., Liebert J., Kirkpatrick J. D., Koerner D. W., Burgasser A. J., 2003, *AJ*, 125, 3302
 Goldreich P., Ward W. R., 1973, *ApJ*, 183, 1051
 Goodman A. A., Benson P. J., Fuller G. A., Myers P. C., 1993, *ApJ*, 406, 528
 Goodwin S. P., Whitworth A., 2007, *A&A*, 466, 943
 Goodwin S. P., Whitworth A. P., Ward-Thompson D., 2004a, *A&A*, 414, 633
 Goodwin S. P., Whitworth A. P., Ward-Thompson D., 2004b, *A&A*, 423, 169
 Goodwin S. P., Hubber D. A., Moraux E., Whitworth A. P., 2005, *Astron. Nachr.*, 326, 1040
 Goodwin S. P., Whitworth A. P., Ward-Thompson D., 2006, *A&A*, 452, 487
 Greaves J. S., 2005, *Astron. Nachr.*, 326, 1044
 Guenther E. W., Paulson D. B., Cochran W. D., Patience J., Hatzes A. P., Macintosh B., 2005, *A&A*, 442, 1031
 Guieu S. et al., 2007, *A&A*, 465, 855
 Hayashi C., Nakano T., 1963, *Prog. Theor. Phys.*, 30, 460
 Heap S. R., Lindler D. J., Lanz T. M., Cornett R. H., Hubeny I., Maran S. P., Woodgate B., 2000, *ApJ*, 539, 435
 Herczeg G. J., Hillenbrand L. A., 2008, *ApJ*, 681, 594
 Hubber D. A., Whitworth A. P., 2005, *A&A*, 437, 113
 Hubeny I., 1990, *ApJ*, 351, 632
 Jayawardhana R., Mohanty S., Basri G., 2003, *ApJ*, 592, 282
 Jensen E. L. N., Mathieu R. D., Donar A. X., Dullighan A., 2004, *ApJ*, 600, 789
 Joergens V., 2006a, *A&A*, 446, 1165
 Joergens V., 2006b, *A&A*, 448, 655
 Joergens V., 2008, preprint (arXiv:0809.3001)
 Johnson B. M., Gammie C. F., 2003, *ApJ*, 597, 131
 Klein R., Apai D., Pascucci I., Henning T., Waters L. B. F. M., 2003, *ApJ*, 593, L57
 Kraus A. L., White R. J., Hillenbrand L. A., 2006, *ApJ*, 649, 306
 Kumar S. S., 1962, Institute for Space Studies Report Number X-644-62-78,

- Kurosawa R., Harries T. J., Littlefair S. P., 2006, *MNRAS*, 372, 1879
- Lafrenière D. et al., 2007, *ApJ*, 670, 1367
- Lafrenière D., Jayawardhana R., van Kerkwijk M. H., 2008, preprint (arXiv:0809.1424)
- Lodato G., Rice W. K. M., 2004, *MNRAS*, 351, 630
- Lodato G., Delgado-Donate E., Clarke C. J., 2005, *MNRAS*, 364, L91
- Low C., Lynden-Bell D., 1976, *MNRAS*, 176, 367
- Lucas P. W., Roche P. F., 2000, *MNRAS*, 314, 858
- Luhman K. L., 2004, *ApJ*, 617, 1216
- Luhman K. L., D'Alessio P., Calvet N., Allen L. E., Hartmann L., Megeath S. T., Myers P. C., Fazio G. G., 2005a, *ApJ*, 620, L51
- Luhman K. L. et al., 2005b, *ApJ*, 631, L69
- Luhman K. L., Adame L., D'Alessio P., Calvet N., Hartmann L., Megeath S. T., Fazio G. G., 2005c, *ApJ*, 635, L93
- Luhman K. L., Joergens V., Lada C., Muzerolle J., Pascucci I., White R., 2007, in Reipurth B., Jewitt D., Keil K., eds, *Protostars and Planets V*. Univ. Arizona Press, Tucson, p. 443
- Makino J., Aarseth S. J., 1992, *PASJ*, 44, 141
- Marcy G. W., Butler R. P., 2000, *PASP*, 112, 137
- Masunaga H., Inutsuka S.-I., 1999, *ApJ*, 510, 822
- Masunaga H., Inutsuka S.-I., 2000, *ApJ*, 531, 350
- Masunaga H., Miyama S. M., Inutsuka S.-I., 1998, *ApJ*, 495, 346
- Matzner C. D., Levin Y., 2005, *ApJ*, 628, 817
- Maxted P. F. L., Jeffries R. D., Oliveira J. M., Naylor T., Jackson R. J., 2008, *MNRAS*, 385, 2210
- Mayer L., Quinn T., Wadsley J., Stadel J., 2004, *ApJ*, 609, 1045
- Mejía A. C., Durisen R. H., Pickett M. K., Cai K., 2005, *ApJ*, 619, 1098
- Mohanty S., Jayawardhana R., Basri G., 2005, *ApJ*, 626, 498
- Monin J.-L., Ménard F., Peretto N., 2006, *A&A*, 446, 201
- Morris J. P., Monaghan J. J., 1997, *J. Comput. Phys.*, 136, 41
- Mundy L. G., Looney L. W., Lada E. A., 1995, *ApJ*, 452, L137
- Muzerolle J., Luhman K. L., Briceño, C., Hartmann L., Calvet N., 2005, *ApJ*, 625, 906
- Najita J. R., Tiede G. P., Carr J. S., 2000, *ApJ*, 541, 977
- Nakajima T., Oppenheimer B. R., Kulkarni S. R., Golimowski D. A., Matthews K., Durrance S. T., 1995, *Nat*, 378, 463
- Natta A., Testi L., Muzerolle J., Randich S., Comerón F., Persi P., 2004, *A&A*, 424, 603
- Oppenheimer B. R., Kulkarni S. R., Matthews K., Nakajima T., 1995, *Sci*, 270, 1478
- Padoan P., Nordlund Å., 2004, *ApJ*, 617, 559
- Payne M. J., Lodato G., 2007, *MNRAS*, 381, 1597
- Pollack J. B., Hubickyj O., Bodenheimer P., Lissauer J. J., Podolak M., Greenzweig Y., 1996, *Icarus*, 124, 62
- Quillen A. C., 2006, *ApJ*, 640, 1078
- Rafikov R. R., 2005, *ApJ*, 621, L69
- Rebolo R., Zapatero-Osorio M. R., Martín E. L., 1995, *Nat*, 377, 129
- Rees M. J., 1976, *MNRAS*, 176, 483
- Reipurth B., Clarke C., 2001, *AJ*, 122, 432
- Riaz B., Gizis J. E., 2007, *ApJ*, 661, 354
- Riaz B., Gizis J. E., 2008, *ApJ*, 681, 1584
- Rice W. K. M., Armitage P. J., Bate M. R., Bonnell I. A., 2003, *MNRAS*, 339, 1025
- Rice W. K. M., Lodato G., Armitage P. J., 2005, *MNRAS*, 364, L56
- Rodríguez L. F., Loinard L., D'Alessio P., Wilner D. J., Ho P. T. P., 2005, *ApJ*, 621, L133
- Safronov V. S., 1969, *Evolution of the Protoplanetary Cloud and Formation of the Earth and Planets*. Nauka, Moscow
- Scholz A., Jayawardhana R., Wood K., 2006, *ApJ*, 645, 1498
- Spiegel E. A., 1957, *ApJ*, 126, 202
- Stamatellos D., Whitworth A. P., 2008, *A&A*, 480, 879
- Stamatellos D., Whitworth A. P., Bisbas T., Goodwin S., 2007a, *A&A*, 475, 37
- Stamatellos D., Hubber D. A., Whitworth A. P., 2007b, *MNRAS*, 382, L30
- Thébaud P., Marzari F., Scholl H., 2006, *Icarus*, 183, 193
- Thies I., Kroupa P., 2007, *ApJ*, 671, 767
- Toomre A., 1964, *ApJ*, 139, 1217
- Udry S., Santos N. C., 2007, *ARA&A*, 45, 397
- Udry S., Mayor M., Queloz D., 2003, in Deming D., Seager S., eds, *ASP Conf. Ser. Vol. 294, Scientific Frontiers in Research on Extrasolar Planets*. Astron. Soc. Pac., San Francisco, p. 17
- Umbreit S., Burkert A., Henning T., Mikkola S., Spurzem R., 2005, *ApJ*, 623, 940
- Whelan E. T., Ray T. P., Bacciotti F., Natta A., Testi L., Randich S., 2005, *Nat*, 435, 652
- Whitehouse S. C., Bate M. R., 2006, *MNRAS*, 367, 32
- Whitworth A. P., Stamatellos D., 2006, *A&A*, 458, 817
- Whitworth A. P., Zinnecker H., 2004, *A&A*, 427, 299
- Whitworth A., Bate M. R., Nordlund Å., Reipurth B., Zinnecker H., 2007, in Reipurth B., Jewitt D., Keil K., eds, *Protostars and Planets V*. Univ. Arizona Press, Tucson, p. 459
- Williams J. P., Andrews S. M., Wilner D. J., 2005, *ApJ*, 634, 495
- Zapatero Osorio M. R., Béjar V. J. S., Martín E. L., Rebolo R., y Navascués D. B., Bailer-Jones C. A. L., Mundt R., 2000, *Sci*, 290, 103

This paper has been typeset from a $\text{\TeX}/\text{\LaTeX}$ file prepared by the author.